

Experimental Investigation of R-22 Condensation in Tubes with Small Inner Diameter

Nae Hyun Kim* and Jin Pyo Cho**

Key Words : Condensation, In-tube, R-22, Small diameter, Heat transfer coefficient, Pressure drop

Abstract

In this study, condensation heat transfer experiments were conducted in two small diameter ($\phi 7.5$, $\phi 4.0$) tubes. Comparison with the existing in-tube condensation heat transfer correlations indicated that these correlations overpredict the present data. For example, Akers correlation overpredicted the data up to 104%. The condensation heat transfer coefficient of the $\phi 4.0$ I.D. tube was smaller than that of the $\phi 7.5$ I.D. tube; at the mass velocity of 300 kg/m²s, the difference was 12%. The pressure drop data of the small diameter tubes were highly (two to six times) overpredicted by the Lockhart-Martinelli correlation. Sub-cooled forced convection heat transfer test confirmed that Gnielinski's single phase heat transfer correlation predicted the data reasonably well.

Nomenclature

A	: heat transfer area [m ²]	g	: gravity [m/s^2]
C_p	: specific heat [J/kgK]	G	: mass velocity [kg/m ² s]
d_i	: tube inner diameter [m]	h	: heat transfer coefficient [equation (13)] [W/m ² K]
D_h	: hydraulic diameter of the annular section [m]	h_{fg}	: latent heat of vaporization [J/kg]
f	: two-phase friction factor [equation (25)]	j_g^*	: dimensionless vapor velocity [equation (20)]
f_l	: liquid friction factor [equation (26)]	k	: thermal conductivity [W/mK]
		L	: length of the test section [m]
		m	: mass flow rate [kg/s]
		Nu_{Dh}	: Nusselt number based on D_h
		Pr	: Prandtl number

* Department of Mechanical Engineering,
University of Incheon, Incheon, Korea

** Graduate School, University of Incheon,
Incheon, Korea

- q : heat flux [W/m²]
 Q : heat transfer rate [W]
 Re_{Dh} : Reynolds number based on Dh
 Re_{eq} : equivalent Reynolds number [equation (22)]
 Re_l : liquid Reynolds number [equation (27)]
 t : wall thickness [m]
 U : overall heat transfer coefficient [W/m²K]
 x : quality
 X_u : Martinelli parameter [equation (19)]

Greek symbols

- α : void fraction
 ΔP : pressure loss across the test section [N/m²]
 ΔT : temperature difference [K]
 μ : viscosity [Ns/m²]
 ρ : density [kg/m³]
 ϕ_v^2 : two-phase friction multiplier [equation (3)]

subscripts

- a : acceleration
 ave : average
 exp : experimental
 eq : equivalent
 f : friction
 i : tube-side
 l : liquid
 lat : latent
 lm : log-mean
 o : tube outside
 p : preheater
 r : refrigerant
 sat : saturation
 $sens$: sensible
 t : total
 v : vapor
 w : water

Until recently, most fin-tube heat exchangers of small air-conditioning units have used ϕ 9.5 (9.5mm tube outer diameter) copper tubes. The recent trend, however, is to use smaller diameter tubes. Air-conditioning units using ϕ 7 heat exchangers are under production, and units with ϕ 4 heat exchangers are known to be under development. For fin-tube heat exchangers, significant portion of the total pressure drop is attributable to the profile drag of the tube, therefore, reduction of the tube diameter will decrease the pressure loss of the heat exchangers. In addition, low thermal performance region behind the tube will also be decreased, which makes the use of small-diameter tube more attractive.

Literature survey revealed that the only limited studies have been conducted for condensation in small-diameter tubes. Dobson⁽¹⁾ conducted condensation tests in ϕ 7.04, ϕ 4.57 and ϕ 3.14 tubes using three different refrigerants including R-22. Yang and Webb⁽²⁾, Katsuda⁽³⁾, Jeon et al.⁽⁴⁾ and Kim⁽⁵⁾ conducted condensation tests in flat aluminum extruded tubes. The flat tubes are commonly used in condensers for car air-conditioning system. They are multi-channel-shaped with the hydraulic diameter of 1~2mm. Dobson⁽¹⁾ reported that the existing condensation correlations reasonably predicted his data. Yang and Webb⁽²⁾, however, reported that their data were overpredicted by the correlations. In this study, R-22 condensation tests were conducted in ϕ 7.5 and ϕ 4.0 tubes with mass flux varying from 150 kg/m²s to 800 kg/m²s, and heat flux from 5 kW/m² to 16 kW/m². These data are compared with existing correlations.

2. Experimental Apparatus

The schematic drawing of the apparatus is

1. Introduction

shown in Fig.1, and details of the test section are shown in Fig.2. The test section is a double-pipe heat exchanger with refrigerant flowing inside and water flowing on the annular-side of the tube. The length is 500mm. It is important to make the thermal resistance on the water-side small, which is accomplished by making the gap width of the annular section small. In this study, the gap is 1.0mm. The geometric dimensions of the test section is shown in Fig2.

As shown in Fig.1, the refrigerant flows into the test section at a known quality. Part of the refrigerant condenses in the test section by the cooling water on the annular-side. The vapor separator located downstream of the test section separates the two-phase refrigerant, sending the vapor to the upper condenser and the liquid into the receiver. Sub-cooled refrigerant in the

receiver is then supplied to the preheater by the magnetic pump. A mass flow meter is located between the pump and the preheater. The refrigerant inlet quality is controlled by the 5 kW preheater. The refrigerant flow rate is controlled by by-passing part of the flow out of the pump. The heat flux into the test tube is controlled by changing the temperature of the cooling water in the annular-side. Thus for the present setup, refrigerant quality, flow rate and heat flux are separately controlled.

The temperature of the cooling water rises as it passes through the annular-side of the test section. The heat is removed at the plate heat exchanger downstream of the test section. The inlet temperature is controlled by the immersion heater in the reservoir and the flow rate is measured by the float-type flow meter located between the pump and the test section. Five temperatures ; refrigerant inlet and outlet, cooling water inlet and outlet, preheater inlet ; are measured by pre-calibrated RTDs. System pressures are measured at two locations ; one at the inlet of the test section, the other at the inlet of the preheater. These pressures are compared with the temperatures measured at the same location, and used to check the refrigerant status(saturated or subcooled). A differential pressure transducer is used to measure the pressure drop across the test section. All the pressure transducers are pre-calibrated using a precision dead weight tester before installation.

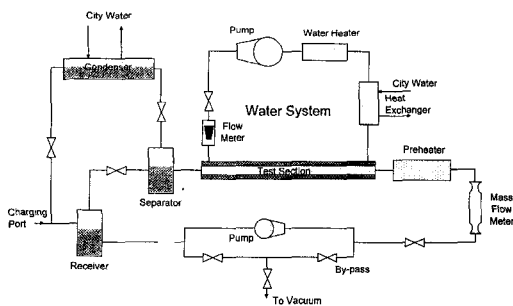
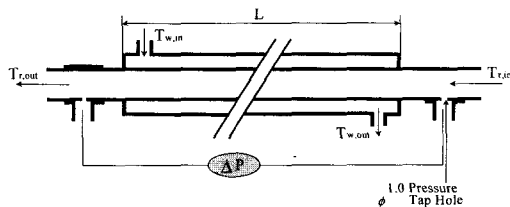


Fig.1 Schematic drawing of the apparatus.



	Type1	Type2
Inner tube I.D	φ 0.4	φ 7.5
Inner tube O.D	φ 6.0	φ 9.5
Outer tube I.D	φ 7.7	φ 10.9
Inner tube material	Stainless steel	Copper
L	0.495m	0.5 m

Fig.2 Schematic details of the test section.

3. Test Method

The apparatus operates at approximately 15 atmospheric pressure, and should be leak-tight. A leak test was conducted using a soap bubble technique followed by a halogen leak test. The

apparatus was fixed several times, and finally the leak was less than 0.5 kPa per hour at 20 atmospheric pressure. It is important to charge an appropriate amount of refrigerant into the system. If the charging is too small, control of the flow rate is difficult and may damage the magnetic pump. If too much refrigerant is charged, control of the system pressure becomes difficult at high heat flux. The amount of charge was determined by trial and error. Before charging the refrigerant, the system was vacuumed for about an hour. Then, small amount of refrigerant was charged in, and flushed out with the remaining air using a vacuum pump. The procedure was repeated several times.

The amount of remnant air in the system may be checked by comparing the measured temperature with the measured pressure. During tests, they matched within 0.3K. The test procedure is as follows.

- (1) Set the refrigerant flow rate at maximum.
- (2) Set the inlet quality of the test section at maximum using a preheater.
- (3) Set the Reynolds number of the cooling water at 2000.
- (4) Set the heat flux into the test section at maximum.
- (5) Repeat the test decreasing the heat flux. Heat flux decreased by lowering the cooling water temperature.
- (6) Repeat the test decreasing the quality.
- (7) Repeat the test decreasing the flow rate.

Test range covered heat flux from 5 kW/m² to 16 kW/m², quality from 0.1 to 0.9, and mass flux from 150 kg/m²s to 800 kg/m²s.

4. Data Reduction

The present test was conducted with the test section at horizontal position. Thus, the

measured pressure loss (ΔP_{exp}) consists of the frictional loss (ΔP_f) and the acceleration loss (ΔP_a), neglecting gravitational loss.

$$\Delta P_{exp} = \Delta P_f + \Delta P_a \quad (1)$$

From the separated flow model(6), ΔP_f and ΔP_a may be expressed as follows.

$$\Delta P_a = -\Delta \left[\frac{G^2 x^2}{\alpha \rho_v} + \frac{G^2 (1-x)^2}{(1-\alpha) \rho_l} \right] \quad (2)$$

$$\Delta P_a = \left(\frac{dp}{dz} \right)_f \Delta z = \Phi_v^2 \left(\frac{dp}{dz} \right)_v \Delta z \quad (3)$$

Here, $(dp/dz)_v$ is the pressure gradient obtained with the gas phase alone flowing in the tube and α is the void fraction, which may be expressed as follow(6,7).

$$\left(\frac{dp}{dz} \right)_v = - \frac{0.079 G^2 x^2}{\rho_v d_i (G x d_i / \mu_v)^{0.25}} \quad (4)$$

$$\alpha = \left[1 + \frac{1-x}{x} \left(\frac{\rho_v}{\rho_l} \right)^{2/3} \right]^{-1} \quad (5)$$

Inserting equations (2), (3) into equation (1) results in Martinelli parameter X_{tt} as a function of two phase friction multiplier Φ_v^2 .

Heat transferred to the test section is obtained as follows.

$$Q_t = m_w c_{pw} (T_{w, out} - T_{w, in}) \quad (6)$$

The refrigerant inlet quality x_{in} is obtained from the energy balance at the preheater. Heat transferred to the preheater consists of a sensible and a latent part.

$$Q_p = Q_{sens} + Q_{lat} \quad (7)$$

$$Q_{sens} = m_r c_{pr} (T_{sat} - T_{p, in}) \quad (8)$$

$$Q_{lat} = m_r h_{fg} x_{in} \quad (9)$$

Then, x_{in} is given by equation (10).

$$x_{in} = \frac{1}{h_{fg}} \left[\frac{Q_p}{m_r} - c_{pr}(T_{sat} - T_{p,in}) \right] \quad (10)$$

The quality change across the test section is given by equation (11).

$$\Delta x = \frac{Q_t}{m \cdot h_{fg}} \quad (11)$$

The average quality in the test section is given by equation (12).

$$x_{ave} = x_{in} - \frac{\Delta x}{2} \quad (12)$$

The condensation heat transfer coefficient is obtained from equation (14) based on the energy balance of the test section.

$$Q_t = U_o A_o \Delta T_m = h_i A_i \Delta T_i = h_o A_o \Delta T_o \quad (13)$$

$$h_i = \frac{1}{\left[\frac{1}{U_o} - \frac{1}{h_o} \right] \frac{A_i}{A_o} - \frac{t A_i}{k A_m}} \quad (14)$$

Here, A_m is the average heat transfer area related with the tube wall conduction. The annular-side heat transfer coefficient h_o is determined from the modified Wilson Plot⁽⁸⁾. In this method, annular-side heat transfer correlation is assumed to be that of Sieder-Tate⁽⁹⁾ type, and exponent of the Reynolds number and proportional constant are determined from the experimental data. Experiments are con-

ducted varying the annular-side flow rate with the tube side flow rate and the temperature fixed. This method is known to have advantage over the original Wilson Plot⁽¹⁰⁾ that smaller numbers of test runs are needed. One should be cautious to make both sides of the flow turbulent. To make the flow of annular-side turbulent, thin wire of $\phi 0.2$ was wrapped around the tube at a pitch of 5mm.

5. Experimental Results.

5.1 Annular-side heat transfer coefficient

Experiments were conducted varying annular-side Reynolds numbers from 1000 to 3000. The water temperature of the annular-side was fixed at 35°C and the tube-side was fixed at 60°C, the water velocity of the tube-side was 6.2 m/s. The typical wilson Plot results are shown in Fig.3. Here, X1 and Y1 are parameters given as follows.

$$X_1 = A_i / [A_o (k_w / D_h) (\text{Re}_{Dh}^m \text{Pr}^{1/3})] \quad (15)$$

$$Y_1 = \left(\frac{1}{U_o A_o} - \frac{t}{k A_m} \right) A_i \quad (16)$$

Two annular-side correlations for the present tubes are as follows.

$$\phi 7.5 : N_{u,ah} = 0.0694 \text{Re}_{Dh}^{0.74} \text{Pr}^{1/3} \quad (17)$$

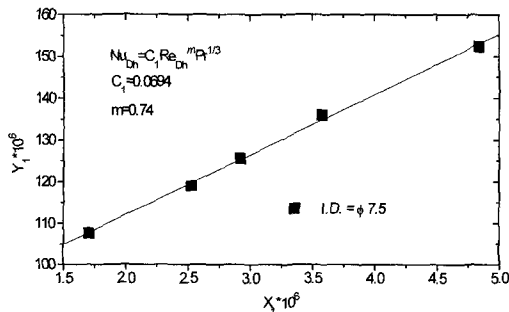


Fig.3 Typical modified Wilson plot.

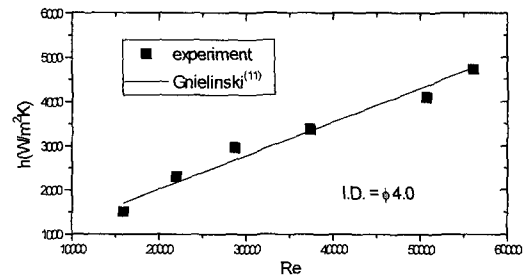


Fig.4 Sub-cooled forced convection heat transfer coefficient of the $\phi 4.0$ tube.

$$\phi 4.0 : N_{u,ph} = 0.0274 Re_{ph}^{0.81} Pr^{1/3} \quad (18)$$

The heat transfer rate of the tube-side matched with that of the annular-side within 5%.

5.2 Sub-cooled heat transfer coefficient

Prior to the condensation tests, sub-cooled heat transfer tests were conducted with R-22 liquid flowing in the tube. Throughout the tests, annular-side water temperature(25°C) and velocity(1.0m/s) were maintained uniform. Figure 4 shows the measured heat transfer coefficient compared with the Gnielinski⁽¹¹⁾ correlation. The data agree with the correlation within 6%.

5.3 Condensation heat transfer coefficient

Condensation tests were conducted for $\phi 7.5$ and $\phi 4.0$ tubes with mass flux from 150 kg/m² s to 800 kg/m² s and heat flux from 5 kW/m² to 16 kW/m². Saturation temperature was maintained at 45°C.

Flow regime

Of the many flow regime maps, that of Breber et al.⁽¹²⁾ was decided to be suitable for the present study. Figure 5 shows the locus of the estimated flow regime at different mass velocities (150, 300, 580, 800 kg/m²s).

Here, X_{tt} is Martinelli parameter and fg^* is dimensionless gas velocity, which are defined

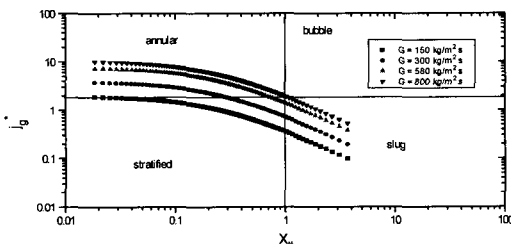


Fig.5 Flow regime map of Breber et al.⁽¹²⁾

as follows.

$$X_u = (\rho_v/\rho_l)^{0.5} (\mu_l/\mu_v)^{0.1} [(1-x)/x]^{0.9} \quad (19)$$

$$j_g^* = \frac{xG}{[gd_l\rho_v(\rho_l-\rho_v)]^{0.5}} \quad (20)$$

Figure 5 shows that, at a mass flux of 150 kg/m²s, stratified flow is dominant. Annular flow is dominant over 580 kg/m²s. At 300 kg/m²s, stratified flow is dominant at a low quality region, and annular flow is dominant at a high quality region.

Condensation pressure drop

Figure 6 shows the pressure gradient for a $\phi 4.0$ tube, where the pressure drop increases as the quality and the mass flux increase. In Fig.7

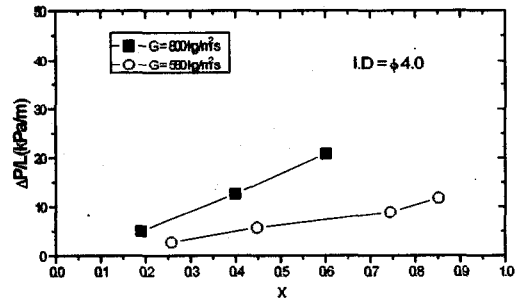


Fig.6 Two-phase flow pressure gradient in the $\phi 4.0$ tube.

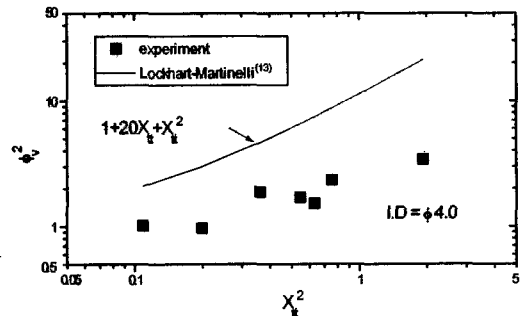


Fig.7 Two-phase friction multiplier in the $\phi 4.0$ tube vs. Martinelli parameter.

the pressure drop data are reduced in the form of two-phase friction multiplier ϕ_v^2 and Martinelli parameter X_{tt} . Figure 7 shows that the Lockhart-Martinelli⁽¹³⁾ correlation considerably overpredicts the data (2 to 6 times). Yang and Webb⁽¹⁴⁾ obtained the similar results from their flat-tube condensation tests. The difference of the tube inlet and outlet quality ranged from 3 to 20%. This difference increased as the mass flux got smaller and the heat flux got larger.

Uncertainty analysis on ϕ_v^2 was conducted following Kline and McClintock⁽¹⁵⁾, which showed $\pm 15.4\%$ at 580 kg/m's and $\pm 8.2\%$ at 800 kg/m's.

Condensation heat transfer coefficient

The condensation heat transfer correlations may be grouped as stratified-flow correlations and annular-flow correlations. The stratified-flow correlations are applicable to gravity-dominated regime at low velocity. Chato⁽¹⁶⁾, Jaster and Kosty⁽¹⁷⁾ developed these correlations. Annular-flow correlations are applicable to a shear-dominated regime at higher velocity, and Traviss et al.⁽¹⁸⁾, Cavallini and Zecchin⁽¹⁹⁾, Shah⁽²⁰⁾, Boyko and Kruzhilin⁽²¹⁾, Akers et al.⁽²²⁾, proposed shear-dominated correlations.

Figure 8 compares the predictions at the present test condition (R-22, saturation temperature 45 °C, $G = 300\text{kg/m}^2\text{s}$, tube inner diameter

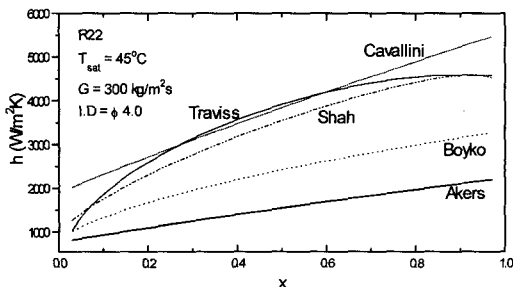


Fig.8 Comparison between different condensation correlations.

$\phi 4.0$), which shows that significant difference exists among the predicted values. The prediction by Traviss et al. is almost twice larger than that by Akers et al. Figure 9 shows the condensation heat transfer coefficients for $\phi 7.5$ tube at 150, 300, 580 kg/m's. The heat flux was maintained at 16 kW/m². The heat transfer coefficient increases as the mass flux and the quality increase. The data are compared with the predictions by previous correlations, where correlations generally overpredict (upto 38%) the data. A similar trend was reported by Yang and Webb⁽²⁾. Uncertainty analysis on the heat transfer coefficient by the method of Kline and McClintock⁽¹⁵⁾ revealed that the error is \pm

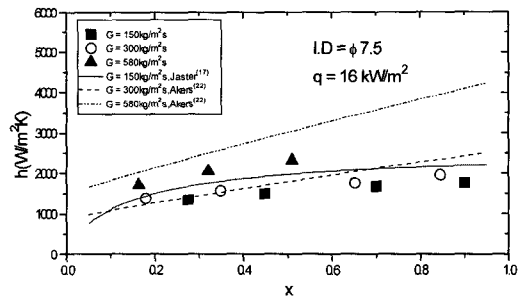


Fig.9 Condensation heat transfer coefficient in the $\phi 7.5$ I.D. tube showing the effect of mass flux.

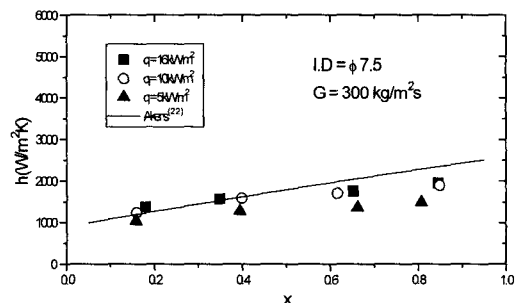


Fig.10 Condensation heat transfer coefficient in the $\phi 7.5$ I.D. tube showing the effect of heat flux.

11.3% at 150kg/m's, and $\pm 6.2\%$ at 800kg/m's.

Figure 10 shows the heat transfer coefficient for different heat fluxes (5, 10, 16 kW/m²) at 300 kg/m's. The heat transfer coefficient slightly increases with the heat flux, which is not consistent with the general notion that the heat transfer coefficient is independent of the heat flux in the annular flow regime. Yang and Webb obtained similar results from the flat-tube tests. At the present time, the reason is not clear. Figure 11 shows the heat transfer coefficient for $\phi 4.0$ tube at different mass flux. Similar trend; the heat transfer coefficient increases as the mass flux and the quality increase; with $\phi 7.5$ tube was noted. Akers et

al.'s correlation overpredicts (up to 68%) the data.

Figure 12 shows the effect of tube diameter. The mass flux was 300 kg/m's and the heat flux was 16 kW/m². The heat transfer coefficient of the $\phi 7.5$ tube is 12% larger than that of the $\phi 4.0$ tube. Figure 13 shows the effect of heat flux at $G = 580$ kg/m's. The heat transfer coefficient slightly increases with the heat flux. Akers et al.'s correlation overpredicts the data up to 104%.

This study reveals that the heat transfer coefficient decreases with the tube diameter. Thus, proper correlation should have the tube diameter as a correlating parameter, where the

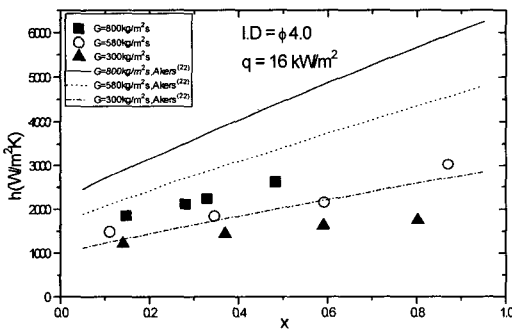


Fig.11 Condensation heat transfer coefficient in the $\phi 4.0$ I.D. tube showing the effect of mass flux.

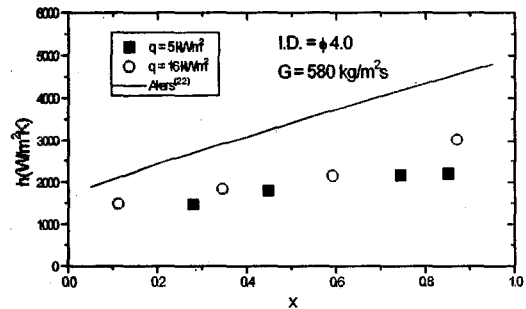


Fig.13 Condensation heat transfer coefficient in the $\phi 4.0$ I.D. tube showing the effect of heat flux.

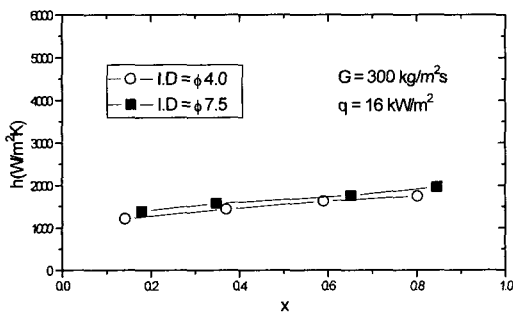


Fig.12 Condensation heat transfer coefficient in the $\phi 4.0$ I.D. tube compared with that in the $\phi 7.5$ I.D. tube.

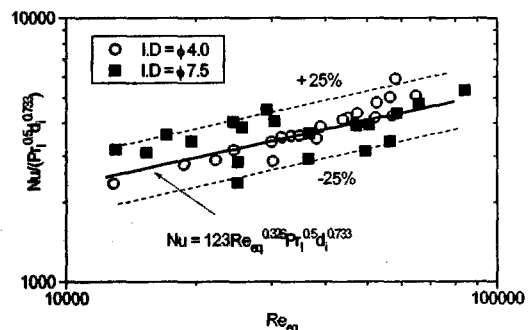


Fig.14 Present data compared with the heat transfer correlation [Equation (21)].

previous correlations were missing. Thus, the new correlation is developed from the present data.

$$Nu = 123 Re_{eq}^{0.326} Pr_i^{0.5} d_i^{0.733} \quad (21)$$

$$Re_{eq} = G_{eq} d_i / \mu_l \quad (22)$$

$$G_{eq} = G_l + G_v (\rho_l / \rho_v)^{0.5} \quad (23)$$

Figure 14 shows that equation⁽²¹⁾ predicts the data within $\pm 25\%$. The pressure drop correlation from this study is given as equation⁽²⁴⁾.

$$f/f_l = 0.0145 Re_{eq}^{0.41} \quad (24)$$

$$f = \frac{\Delta P_f}{4} \frac{d_i}{L} \frac{2\rho_l}{G_{eq}^2} \quad (25)$$

$$f_l = \frac{\Delta P_{f,l}}{4} \frac{d_i}{L} \frac{2\rho_l}{G^2} = 0.079 Re_l^{0.25} \quad (26)$$

$$Re_l = G d_i / \mu_l \quad (27)$$

6. Conclusion

In this study, in-tube condensation tests were conducted for $\phi 7.5$ and $\phi 4.0$ tubes using R-22. Listed below are major findings.

(1) The previous correlations overpredict the present data. Compared with Akers et al.'s correlation, the data are overpredicted up to 104%. The difference increases with the mass flux and the quality.

(2) The heat transfer coefficient of the $\phi 4.0$ tube was smaller than that of the $\phi 7.5$ tube. At a mass flux of 300 kg/m's, the difference was 12%.

(3) Lockhart-Martinelli's correlation overpredicts the present pressure drop data up to 6 times.

(4) The present data are correlated as equations (21) and (24).

References

- (1) Dobson, M. K., 1994, *Heat Transfer and Flow Regimes during Condensation in Horizontal Tubes*, Ph.D Thesis, University of Illinois at Urbana-Champaign.
- (2) Yang, C-J. and Webb, R.L., 1996, "Condensation of R-12 in Small Hydraulic Diameter Extruded Aluminum Tubes with and without Microfins," *Int. J. Heat Mass Trans.*, Vol. 39, No. 4, pp. 791-800.
- (3) Katsuta, M., 1994, "The Effect of a Cross-Sectional Geometry on the Condensation Heat Transfer inside Multi-Pass Tubes," *Proc. of WTPF*, Vol. 2, pp. 146-157, AFERC, POSTECH.
- (4) Jeon, C. D., Chung, J. W. and Lee, J. H., 1997, "Experiments on Condensation Heat Transfer and Pressure Drop Characteristics in the Multi-Channel Flat Tube," *Journal of Society of Air-Conditioning and Refrigeration*, Vol. 9, No. 3, pp. 376-388 (in Korean)
- (5) Kim, J. S., 1996, "Condensing Heat Transfer and Pressure Drop of HFC-134a inside a Flat Extruded Aluminum Tube," *Proceedings of the 1996 spring conference(B)*, KS ME, pp. 755-762 (in Korean)
- (6) Collier, J. G., and Thome, J. R., 1994, *Convective Boiling and Condensation*, Oxford University Press.
- (7) Zivi, S. M., 1964. "Estimation of Steady State Steam Void-Fraction by Means of Principle of Minimum Entropy Production," *Transactions ASME*, Series C, 86, pp. 237-252.

- (8) Wilson, E. E., 1915, "A Basis for Rational Design of Heat Transfer Apparatus," *Trans. ASME*, Vol. 37, pp. 47-70.
- (9) Farrell, P., Wert, K., and Webb, R., 1991, "Heat Transfer and Friction Characteristics of Turbulent Radiator Tubes," *SAE Technical Paper series*, No. 910197.
- (10) Sieder, E. N. and Tate, G. E., 1936, "Heat Transfer and Pressure Drop of Liquids in Tubes," *Ind. Eng. Chem.*, Vol. 28, pp. 1429-1435.
- (11) Gnielinski, V., 1976, "New Equations for Heat and Mass Transfer in Turbulent Pipe Flows," *Int. Chem. Eng.*, Vol. 16, pp. 359-368.
- (12) Breber, G., Palen, J. W. and Taborek, J., 1980, "Prediction of Horizontal Tubeside Condensation of Pure Components Using Flow Regime Criteria," *J. Heat Transfer*, Vol. 102, pp. 471-476.
- (13) Lockhart R. W. and Martinelli, R. C., 1949, "Proposed Correlation of Data for Isothermal Two-Phase, Two-Component Flow in Pipes," *Chem. Eng. Prog.*, Vol. 45, No. 1, pp. 39.
- (14) Yang, C-Y. and Webb, R. L., 1996, "Friction Pressure Drop of R-12 in Small Hydraulic Diameter Extruded Aluminum Tubes with and without Microfins," *Int. J. Heat Mass Trans.*, Vol. 39, No. 4, pp. 801-809.
- (15) Kline, S. J. and McCintock, F. A., 1953, "The Description of Uncertainties in Single Sample Experiments," *Mechanical Engineering*, Vol. 75, pp. 3-9.
- (16) Chato, J. C., 1962, "Laminar Condensation inside Horizontal and Inclined Tubes," *J. Am. Soc. Heating Refrig. Aircond. Engrs.*, Vol. 4, pp. 52.
- (17) Jaster, H., and Kosky, P. G., 1976, "Condensation in a Mixed Flow Regime," *Int. J. Heat and Mass Transfer*, Vol. 19, pp. 95-99.
- (18) Traviss, D.P., Rohsenow, W. M., and Baron, A. B., 1973. "Forced-Convection Condensation inside Tubes," *ASHRAE Transactions*, Vol. 79, Pt.1, p.157-165.
- (19) Cavallini, A., and Zecchin, R., 1971, "High Velocity Condensation of Organic Refrigerants inside Tubes," *Proceedings of 8th International Congress of Refrigeration*, Brussels, Belgium, Vol. 2, pp. 193-200.
- (20) Shah, M. M., 1979. "A General Correlation for Heat Transfer during Film Condensation in Tubes," *Int. J. Heat Mass Transfer*, Vol. 22, No. 4, pp. 547-556.
- (21) Boyko, L. D. and Kruzhilin, G. N., 1967, "Heat Transfer and Hydraulic Resistance during Condensation of Steam in a Horizontal Tube and in a Bundle of Tubes," *Int. J. Heat Mass Trans.*, Vol. 10, pp. 361-373.
- (22) Akers, W. W., Deans, H. A., and Crosser, O. K., 1958. "Condensation Heat Transfer within Horizontal Tubes," *Chemical Engineering Progressive Symposium Series*, Vol. 55, No. 29, pp. 171-176.